Adsorption of Methane, Nitrogen, Carbon Dioxide, and Their Binary Mixtures on Dry Activated Carbon at 318.2 K and Pressures up to 13.6 MPa

Mahmud Sudibandriyo, Zhejun Pan, James E. Fitzgerald, Robert L. Robinson Jr., and Khaled A. M. Gasem*

School of Chemical Engineering, 423 EN, Oklahoma State University, Stillwater, Oklahoma 74078

Received December 18, 2002. In Final Form: March 27, 2003

A detailed experimental study has been made of the adsorption of pure methane, nitrogen, carbon dioxide, and their binary mixtures on dry activated carbon (Filtrasorb 400, 12 × 40 mesh, Calgon Carbon) at 318.2 K and pressures up to 13.6 MPa. The mixture measurements were made at nominal feed-gas compositions of 20, 40, 60, and 80 mol %. The mixture data clearly elucidate the competitive nature of the individual-component adsorption from the mixtures. Measurements were made using a volumetric technique, coupled with gas chromatographic analysis of the equilibrium gas-phase compositions. Error propagation analysis reveals the expected average experimental uncertainties in the amount adsorbed of 2% for pure methane and nitrogen and 6% for CO_2. For the mixture measurements, the uncertainties are estimated to be about 3% for the total adsorption, while the individual-component uncertainties vary from 0.02 to 0.2 mmol/g activated carbon, depending on the mixture composition. The data were correlated using the two-dimensional Zhou−Gasem−Robinson equation of state model. The model fits the pure-component adsorption data within their experimental uncertainties, whereas the total and individual-component adsorptions in the binary systems are represented within one to two times the expected experimental uncertainties. As an additional benefit, the good agreement between the present data and those of Humayun and Tomasko for pure carbon dioxide (using two very different experimental techniques) suggests that these data provide a useful reference for benchmarking new experimental apparatus/techniques intended for the high-pressure adsorption measurements of supercritical gases.

1. Introduction

The authors' long-range objective is to develop reliable models to predict the adsorption behavior of supercritical gases on coals, with specific applications to (a) coalbed methane production and (b) the use of coalbeds to sequester the greenhouse gas carbon dioxide. In pursuit of that objective, we have performed both experimental[1] and modeling[2−5] studies.

Evaluating mathematical models to describe adsorption behavior on coals is complicated by (a) the difficulty in characterizing the coal matrix adequately and (b) assessing the effect of water (found in essentially all coalbeds) on the adsorption behavior. As a result, we decided to perform studies on a more readily characterized carbon matrix and in the absence of water. This led to the choice of dry activated carbon for the present study. Our rationale is that useful models should be expected to fit the data on activated carbon prior to extending them to include the effects of the complex adsorbent structure of coals and the presence of water.

An added incentive was the fact that Humayun and Tomasko[6] recently measured the adsorption of carbon dioxide on activated carbon using a gravimetric method. Combined, their data and ours could be used to confirm the mutual viability of the two experimental techniques employed. This is especially useful because the gravimetric technique involves different experimental considerations than the volumetric method of our work.

Several theories and models have been developed to correlate high-pressure pure-adsorption data and to predict gas mixture adsorption. In this study, we used the two-dimensional Zhou−Gasem−Robinson (2-D ZGR) equation of state (EOS) to demonstrate its ability to correlate the experimental data. More general, detailed evaluations of the ZGR EOS and other models (e.g., Ono−Kondo and simplified local density) for adsorption on activated carbon and coals will soon appear elsewhere.[7,8]

* Author to whom correspondence should be addressed. Fax: (405) 744−6338. Telephone: (405) 744−7960. E-mail: gasem@okstate.edu.

(1) Hall, F.; Zhou, C.; Gasem, K. A. M.; Robinson, R. L., Jr. Adsorption of Pure Methane, Nitrogen, and Carbon Dioxide and Their Binary Mixtures on Wet Fruitland Coal, *SPE Paper 29194*. Presented at the Eastern Regional Conference & Exhibition, Charleston, SC, Nov 8−10, 1994.

(2) Zhou, C.; Hall, F.; Gasem, K. A. M.; Robinson, R. L., Jr. Predicting Gas Adsorption Using Two-Dimensional Equations of State. *I&EC Research* **1994**, *33*, 1280−1289.

(3) Gasem, K. A. M.; Sudibandriyo, M.; Fitzgerald, J. E.; Pan, Z.; Robinson, R. L., Jr. Measurement and Modeling of Gas Adsorption on Selected Coalbeds. Presented at the AIChE Spring National Meeting, New Orleans, LA, Mar 10−16, 2002.

(4) Gasem, K. A. M.; Fitzgerald, J. E.; Pan, Z.; Sudibandriyo, M.; Robinson, Jr., R. L. Modeling of Gas Adsorption on Coalbeds. *Proceedings of the Eighteenth Annual International Pittsburgh Coal Conference*, Newcastle, Australia, Dec 3−7, 2001.

(5) Pan, Z.; Sudibandriyo, M.; Fitzgerald, J. E.; Robinson, R. L., Jr.; Gasem, K. A. M. Equilibrium Models for Coalbed Methane Production and Carbon Dioxide Sequestration. Presented at the 2002 International Petroleum Environmental Consortium (IPEC) Conference, Albuquerque, NM, Oct 21−25, 2002.

(6) Humayun, R.; Tomasko, D. L. High-Resolution Adsorption Isotherms of Supercritical Carbon Dioxide on Activated Carbon. *AIChE J.* **2000**, *46*, 2065−2075.

(7) Fitzgerald, J. E.; Sudibandriyo, M.; Pan, Z.; Robinson, R. L., Jr.; Gasem, K. A. M. Modeling the Adsorption of Pure Gases on Coals with the SLD Model. *Carbon*, submitted for publication.

(8) Fitzgerald, J. E.; Sudibandriyo, M.; Pan, Z.; Robinson, R. L., Jr.; Gasem, K. A. M. Comparison of Models for Representing Mixture Adsorption on Coals. To be submitted for publication.

10.1021/la020976k CCC: $25.00
Published on Web 05/29/2003

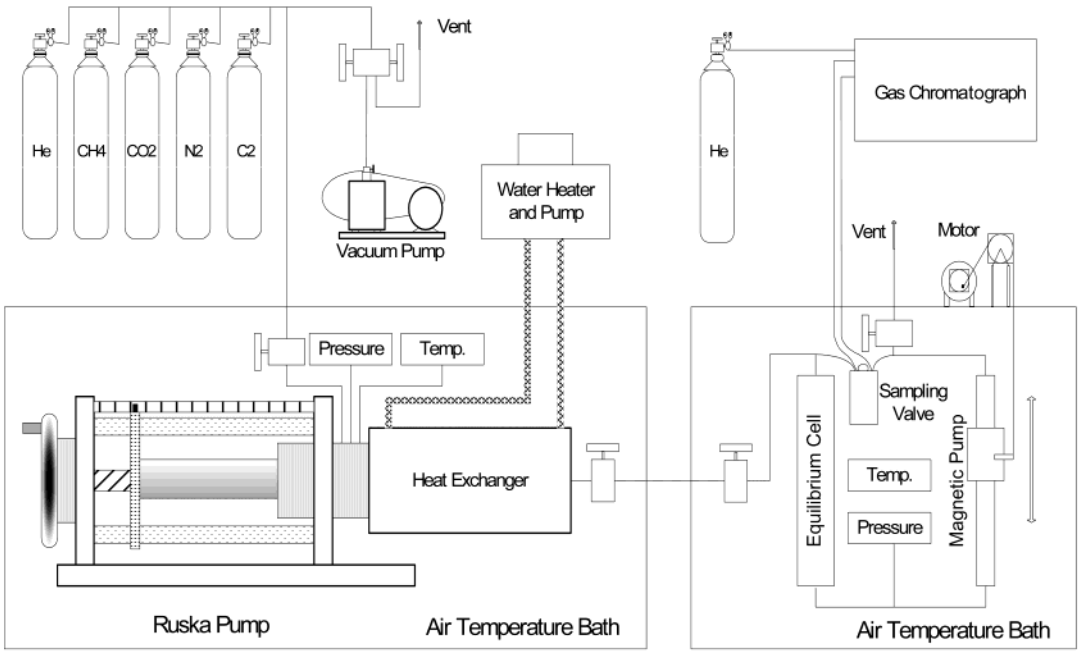

Figure 1. Schematic diagram of the experimental apparatus.

2. Experimental Methods and Procedures

2.1. Adsorption Measurements. The experimental method is based on a mass balance principle, which employs precise measurements of pressures, volumes, and temperatures. A brief description of the apparatus and procedures follows.

The experimental apparatus, shown schematically in Figure 1, has been used successfully in previous studies.[1] The pump and cell sections of the apparatus are maintained in two constant temperature air baths at 318.2 K. The equilibrium cell has a volume of 110 cm^3 and is filled with the adsorbent to be studied. The cell is placed under vacuum prior to the gas injection. The void volume V_{void} in the equilibrium cell is then determined by injected known quantities of helium from a calibrated injection pump (Ruska Pump). Because helium is not significantly adsorbed, the void volume can be determined from the measured values of the temperature, pressure, and amount of helium injected into the cell. Several injections made into the cell at different pressures show consistency in the calculated void volume. Generally, the void volume calculated from sequential injections varies less than 0.3 cm^3 from the average value (of approximately 100 cm^3) on the basis of at least five injections. The mass-balance equation, expressed in volumetric terms, is

$$V_{void} = \frac{\left(\frac{P\Delta V}{ZT}\right)_{pump}}{\left(\frac{P_2}{Z_2T} - \frac{P_1}{Z_1T}\right)_{cell}} \quad (1)$$

where ΔV is the volume injected from the pump, Z is the compressibility factor of helium, T is the temperature, P is the pressure, the subscripts "cell" and "pump" refer to the conditions in the cell and pump sections of the apparatus, respectively, and "1" and "2" refer to conditions in the cell before and after the injection of gas from the pump, respectively. During each injection step, the pressure in the pumps at the end of the injection is adjusted to the initial value, about 6.8 MPa (although the pressures in the pumps during the injection may vary). The void volume from these measurements is then used in the subsequent measurements of adsorption, as follows.

The Gibbs adsorption (also known as the excess adsorption) can be calculated directly from experimental quantities. For the pure-gas adsorption measurements, a known quantity, n_{inj}, of gas (e.g., methane) is injected from the pump section into the cell section. Some of the injected gas will be adsorbed, and the remainder, n_{unads}^{Gibbs}, will exist in the equilibrium bulk (gas) phase in the cell. A molar balance is used to calculate the amount adsorbed, n_{ads}^{Gibbs}, as

$$n_{ads}^{Gibbs} = n_{inj} - n_{unads}^{Gibbs} \quad (2)$$

The amount injected can be determined from the pressure, temperature, and volume measurements of the pump section:

$$n_{inj} = \left(\frac{P\Delta V}{ZRT}\right)_{pump} \quad (3)$$

The amount of unadsorbed gas is calculated from the conditions at equilibrium in the cell:

$$n_{unads}^{Gibbs} = \left(\frac{PV_{void}}{ZRT}\right)_{cell} \quad (4)$$

In eqs 3 and 4, Z is the compressibility of the pure gas at the applicable conditions of the temperature and pressure.

The above steps are repeated at sequentially higher pressures to yield a complete adsorption isotherm. The amount adsorbed is usually presented as an intensive quantity (mmol adsorbed/g adsorbent or mmol/g) by dividing n_{ads}^{Gibbs} by the mass of adsorbent in the cell. Inspection of eqs 2−4 reveals that the amount adsorbed may be calculated in a straightforward manner from the experimental measurements of the pressures, temperatures, and volumes, coupled with the independent knowledge of the gas compressibility factors, Z (from the experimental data or a suitably accurate EOS).

For mixed-gas adsorption measurements, a volumetrically prepared gas mixture of known composition (z_i) is injected; thus, the total amount of each component in the cell is known. A magnetic pump is used to circulate the fluid mixture to ensure that equilibrium is reached. The composition (y_i) of the gas phase in the cell at equilibrium is determined by chromatographic analysis. A pneumatically controlled sampling valve, contained in the air bath at the cell temperature, sends a 20-μL sample to the gas chromatograph (GC) for analysis. The amount of each individual component adsorbed is calculated using component material balances; for component i in the mixture, the relations are

$$n_{ads(i)}^{Gibbs} = n_{inj(i)} - n_{unads(i)}^{Gibbs} = n_{inj}z_i - n_{unads}^{Gibbs}y_i \quad (5)$$

where

$$n_{\mathrm{inj}(i)} = \left(\frac{P\Delta V}{ZRT}\right)_{\mathrm{pump}} z_i \tag{6}$$

and Z is the compressibility of the *feed* gas mixture at the pump conditions, and

$$n^{\mathrm{Gibbs}}_{\mathrm{unads}(i)} = \left(\frac{PV_{\mathrm{void}}}{ZRT}\right)_{\mathrm{cell}} y_i \tag{7}$$

where Z is the compressibility of the *equilibrium* gas mixture at the cell conditions.

2.2. Relationship between Gibbs and Absolute Adsorptions. Adsorption data may also be reported in terms of *absolute* adsorption. The calculations for the Gibbs and absolute adsorptions differ in the manner by which n_{unads} is calculated. The Gibbs adsorption calculation, described above, neglects the volume occupied by the adsorbed phase in calculating the amount of unadsorbed gas (i.e., in eq 4, the entire void volume, V_{void}, is viewed as being available to the unadsorbed gas).

Following is a discussion to clarify the relationships between the Gibbs and absolute adsorptions and to highlight the approximate nature of the calculated absolute adsorption. In addition, expressions are presented that facilitate the calculation of the absolute component adsorption, $n^{\mathrm{Abs}}_{\mathrm{ads}(i)}$, and the adsorbed-phase mole fraction, x_i^{Abs}, in terms of the experimental Gibbs adsorption results.

Pure-Component Adsorption. First, consider the various volumes that can be used to characterize the state existing in the equilibrium cell. When a representation that envisions two distinct, homogeneous fluid phases (bulk gas and adsorbed phase) is used, the total system volume V_{total} of the experimental apparatus is the sum of the volumes of the solid adsorbent (V_{solid}), gas (V_{gas}), and adsorbed-phase (V_{ads}), as follows:

$$V_{\mathrm{total}} = V_{\mathrm{solid}} + V_{\mathrm{gas}} + V_{\mathrm{ads}} \tag{8}$$

The void volume, having been determined by helium injection, is related to these quantities, as follows:

$$V_{\mathrm{void}} = V_{\mathrm{gas}} + V_{\mathrm{ads}} = V_{\mathrm{total}} - V_{\mathrm{solid}} \tag{9}$$

Now, consider the amount of material adsorbed at equilibrium, which may be written in molar terms, as follows:

$$n_{\mathrm{ads}} = n_{\mathrm{total}} - n_{\mathrm{unads}} \tag{10}$$

The difference in the definitions of the Gibbs and total adsorptions resides in the manner in which n_{unads} is related to the volume terms. As was stated previously, in the Gibbs calculation, the volume occupied by the condensed phase is neglected in calculating n_{unads} and the amount of unadsorbed gas is calculated using the entire void volume; thus, using eq 9 for V_{void}, eq 10 becomes

$$n^{\mathrm{Gibbs}}_{\mathrm{ads}} = n_{\mathrm{total}} - V_{\mathrm{void}}\rho_{\mathrm{gas}} \tag{11}$$

where ρ denotes density. In the calculation of the absolute adsorption, n_{unads} is determined using the volume actually available to the bulk gas phase (accounting for the reduction of the volume accessible to the gas as a result of the volume occupied by the adsorbed phase):

$$n^{\mathrm{Abs}}_{\mathrm{ads}} = n_{\mathrm{total}} - V_{\mathrm{gas}}\rho_{\mathrm{gas}} \tag{12}$$

When eqs 11 and 12 are combined to eliminate n_{total}, the following relation between the Gibbs and the absolute adsorptions is obtained:

$$n^{\mathrm{Gibbs}}_{\mathrm{ads}} = n^{\mathrm{Abs}}_{\mathrm{ads}} - V_{\mathrm{ads}}\rho_{\mathrm{gas}} \tag{13}$$

The volume of the adsorbed phase may be expressed in terms of the amount adsorbed and the density of the adsorbed phase as

$$V_{\mathrm{ads}} = n^{\mathrm{Abs}}_{\mathrm{ads}}/\rho_{\mathrm{ads}} \tag{14}$$

Combining eqs 13 and 14 yields

$$n^{\mathrm{Gibbs}}_{\mathrm{ads}} = V_{\mathrm{ads}}(\rho_{\mathrm{ads}} - \rho_{\mathrm{gas}}) \tag{15}$$

Equation 15 clearly illustrates the physical interpretation of the Gibbs adsorption, namely, the amount adsorbed in excess of that which would be present if the adsorbed-phase volume were filled with bulk gas. Combining eqs 14 and 15 leads to

$$n^{\mathrm{Abs}}_{\mathrm{ads}} = n^{\mathrm{Gibbs}}_{\mathrm{ads}}\left(\frac{\rho_{\mathrm{ads}}}{\rho_{\mathrm{ads}} - \rho_{\mathrm{gas}}}\right) \tag{16}$$

An important consideration in the calculation of the absolute adsorption is that it requires knowledge of the adsorbed phase density, ρ_{ads}, which is not readily accessible by an experimental measurement. Thus, estimates of ρ_{ads} are usually employed. A commonly used approximation is the liquid density at the atmospheric pressure boiling point, as was done by Arri and Yee.[9] In this study, however, we used model-regressed estimates for the adsorbed-phase density, as is discussed in section 3.

Adsorption from Mixtures. For absolute adsorption, the component mole fractions in the adsorbed phase, x_i^{Abs}, may be calculated from the component Gibbs adsorptions; however, this requires some assumption regarding the density, ρ_{ads}, of the adsorbed phase *mixture*. In the following discussion, ρ_{ads} is approximated using the assumption of ideal mixing in the adsorbed phase, where the pure-component adsorbed-phase density estimates are used to calculate the mixture adsorbed-phase density. The component Gibbs adsorption (amount of component i in the adsorbed phase in excess of the amount that would be present if the bulk equilibrium gas mixture occupied the volume of the adsorbed phase) may be written using a component material balance as

$$n^{\mathrm{Gibbs}}_{\mathrm{ads}(i)} = n^{\mathrm{Abs}}_{\mathrm{ads}}x_i^{\mathrm{Abs}} - V_{\mathrm{ads}}\rho_{\mathrm{gas}}y_i = V_{\mathrm{ads}}(\rho_{\mathrm{ads}}x_i^{\mathrm{Abs}} - \rho_{\mathrm{gas}}y_i) \tag{17}$$

For convenience, we define a fractional component Gibbs adsorption, $\theta_i^{\mathrm{Gibbs}}$, as

$$\theta_i^{\mathrm{Gibbs}} \equiv n^{\mathrm{Gibbs}}_{\mathrm{ads}(i)}/n^{\mathrm{Gibbs}}_{\mathrm{ads}} \tag{18}$$

(Note that, although eq 18 has the appearance of a mole fraction, the Gibbs adsorption is an excess quantity, not a total quantity for a specified phase; thus, θ, rather than x, is used to denote the quantity.)

Inserting this definition into eq 17, we obtain

$$n^{\mathrm{Gibbs}}_{\mathrm{ads}}\theta_i^{\mathrm{Gibbs}} = n^{\mathrm{Abs}}_{\mathrm{ads}}\left(x_i^{\mathrm{Abs}} - y_i\frac{\rho_{\mathrm{gas}}}{\rho_{\mathrm{ads}}}\right) \tag{19}$$

The combination of eq 16 with eq 19 yields

$$x_i^{\mathrm{Abs}} = \theta_i^{\mathrm{Gibbs}}\left(1 - \frac{\rho_{\mathrm{gas}}}{\rho_{\mathrm{ads}}}\right) + y_i\left(\frac{\rho_{\mathrm{gas}}}{\rho_{\mathrm{ads}}}\right) \tag{20}$$

Equation 20 reveals that x_i^{Abs} and $\theta_i^{\mathrm{Gibbs}}$ become identical in the limit of low pressure (where ρ_{gas} becomes small).

Inspection of eq 20 reveals that all the quantities on the right-hand side can be obtained directly from experimental measurements except for ρ_{ads}, for which some approximation must be made. If ideal mixing is used to represent ρ_{ads} in terms of the pure-component adsorbed-phase densities, we have

$$\frac{1}{\rho_{\mathrm{ads}}} = \frac{x_1^{\mathrm{Abs}}}{\rho_{\mathrm{ads}(1)}} + \frac{x_2^{\mathrm{Abs}}}{\rho_{\mathrm{ads}(2)}} \tag{21}$$

where the subscripts "1" and "2" refer to pure components. Then,

(9) Arri, L. E.; Yee, D. Modeling Coalbed Methane Production with Binary Gas Sorption, *SPE Paper 24363*. Presented at the SPE Rocky Mountain Regional Meeting, Casper, WY, May 18−21, 1992.

eq 20 may be written as

$$x_1^{Abs} = 1 - x_2^{Abs} = \frac{\theta_1^{Gibbs}\rho_{ads(2)} + \rho_{gas}(y_1 - \theta_1^{Gibbs})}{\rho_{ads(2)} + \rho_{gas}(y_1 - \theta_1^{Gibbs})(1 - \rho_{ads(2)}/\rho_{ads(1)})} \quad (22)$$

and the absolute component adsorption can be calculated as follows:

$$n_{ads(i)}^{Abs} = n_{abs}^{Abs} x_i^{Abs} \quad (23)$$

with the use of eq 16 to calculate the *total* mixture adsorption, n_{ads}^{Abs}, where the densities, ρ_{ads} and ρ_{gas}, refer to mixtures of compositions x_i^{Abs} and y_i, respectively.

2.3. Gas Compressibility Factors. As is indicated by eqs 3−7, accurate gas-phase compressibility (Z) factors are required for methane, nitrogen, carbon dioxide, and their mixtures to properly analyze the experimental data. The compressibility factors for pure methane, nitrogen, and carbon dioxide were determined from highly accurate equations of state.[10−12] For the void volume determination, the helium compressibility factor is given by[13]

$$Z_{He} = 1 + (0.001\,471 - 0.000\,004\,779T + 0.000\,000\,004\,92T^2)/P \quad (24)$$

where T is in Kelvin and P is in atmospheres. This expression is based on the experimental data from National Bureau of Standards Technical Note 631 for helium.

A careful evaluation of the current literature led us to conclude that an adequate predictive capability for the mixture Z factors did not exist. Therefore, we elected to use the available pure-fluid and binary-mixture data to refit the Benedict−Webb−Rubin (BWR) EOS and improve its accuracy significantly. In general, the new BWR parameters yield deviations in the Z factors of less than 0.5%. This allowed us to address our compressibility-factor needs for the binary adsorption mixtures. Details of the BWR equation expressions are given elsewhere.[14]

2.4. Materials. The pure gases used in this work were obtained from Airgas−Pennsylvania with reported purities of about 99.99% and were used as received. A bituminous-coal-based activated carbon (Filtrasorb 400, 12 × 40 mesh, Calgon Carbon) was used as the adsorbent; its compositional analysis is presented in Table 1. The composition of the activated carbon is less complex than that of coals. In particular, it has a higher carbon content (ultimate and proximate) and significantly less volatile matter than do typical coals, leading to a less complex characterization problem when interpreting the solid−fluid interactions in the adsorption process. The activated carbon was washed in demineralized water and then dried under vacuum at 230 °F for 2 days before being used in the adsorption measurements. The nitrogen BET surface area at 77 K has been reported to be 850 m^2/g.[6]

2.5. Calibrations. Calibrations were performed routinely during the course of the experiments. The temperature measuring devices were calibrated against a Minco platinum resistance reference thermometer, and the pressure transducers were calibrated against a Ruska deadweight tester with a calibration traceable to the National Institute of Science and Technology.

Table 1. Analysis of Calgon Activated Carbon Used in This Study

analysis	units	value	lower limit	upper limit
Manufacturer Specification[a]				
abrasion number		87	75	
apparent density	g/cm^3	0.53	0.44	
skeleton density	g/cm^3	2.02		
ash	%	7		9
effective size	mm	0.64	0.55	0.75
iodine number	mg/g	1046	1000	
US sieve series on 12	%	1		5
US sieve series −40 Mesh	%	1		4
Ultimate[b]				
carbon	%	88.65		
hydrogen	%	0.74		
oxygen	%	3.01		
nitrogen	%	0.40		
sulfur	%	0.73		
ash	%	6.47		
Proximate[b]				
vol. matter	%	3.68		
fixed carbon	%	89.85		
ash	%	6.47		

[a] Calgon Carbon Corp., Pittsburgh, PA. [b] Huffman Laboratories, Inc., Golden, CO.

The GC was calibrated against volumetrically prepared mixtures at the nominal feed-gas concentrations. The GC used for the composition analysis is a Varian Chrompack CP-3800 with the helium carrier gas maintained at a 0.25-mL/s flow rate. A 10-ft Haysep D packed column was used for the CH_4/CO_2 and N_2/CO_2 systems, and a molecular sieve 13X column was used for the CH_4/N_2 system; the column temperature was 80 °C. A thermal-conductivity detector was used for all of the binary systems studied; its bath temperature was set at 100 °C. The chromatographic response factor, defined as $(A_2/A_1)(y_1/y_2)$, where A is the GC response area, was found to depend slightly on the pressure; as such, the GC was calibrated for each nominal composition at pressure intervals of 1.4 MPa.

The uncertainties in the experimentally measured quantities after the calibrations were estimated as follows: temperatures, 0.1 K; pressures, 6.9 kPa; injected-gas volumes, 0.02 cm^3; gas-mixture compositions, 0.002 mole fraction.

A detailed error propagation analysis was performed, which indicates that the average uncertainties for the pure-adsorption measurements are approximately 1.8% (0.065−0.069 mmol/g) for the methane adsorption, 2.3% (0.054−0.056 mmol/g) for the nitrogen adsorption, and 6.4% (0.269−0.342 mmol/g) for the CO_2 adsorption. The higher percentage of uncertainty for CO_2 is due mainly to the lower value of the Gibbs adsorption for CO_2 at the higher pressure and the higher uncertainty in the CO_2 compressibility factor (due to its proximity to its critical point).

The uncertainties for the binary-mixture adsorptions vary with the composition. The uncertainties for all the binary-gas *total* adsorption measurements are within 4%. The percent of uncertainty of the component gas adsorption, however, can become high at low concentrations of the less-adsorbed gases (i.e., nitrogen in the nitrogen/CO_2 system). Table 2 presents the estimated uncertainties for the mixed-gas adsorption measurements.

3. Experimental Results

3.1. Pure-Gas Adsorption. The experimental data for the pure-gas adsorptions are listed in Tables 3−5. Two independent sets of measurements (runs 1 and 2) for each component were performed to confirm the reproducibility of the data. The results, shown in Figure 2, verify the reproducibility of our procedures because the replicate measurements agree within the expected experimental uncertainties.

Figure 2 presents both the Gibbs and absolute-adsorption behaviors of methane, nitrogen, and CO_2 on activated carbon. Both methane and CO_2 exhibit maxima in the

(10) Span, R.; Wagner, W. A. New Equation of State for Carbon Dioxide Covering the Fluid Region from the Triple Point Temperature to 1100 K at Pressures up to 800 MPa. *J. Phys. Chem. Ref. Data* **1996**, *25*, 1509−1590.

(11) Angus, S.; Armstrong, B.; de Reuck, K. M. *International Thermodynamic Tables of the Fluid State-5: Methane*; IUPAC Chemical Data Series No.16; Pergamon Press: New York, 1978.

(12) Angus, S.; de Reuck, K. M.; Armstrong, B. *International Thermodynamic Tables of the Fluid State-6: Nitrogen*; IUPAC Chemical Data Series No.20; Pergamon Press: New York, 1979.

(13) Hall, F. E. Adsorption of Pure and Multicomponent Gases on Wet Fruitland Coal. M.S. Thesis, Oklahoma State University, 1993.

(14) Bishnoi, P. R.; Robinson, D. B. Mixing Rules Improve BWR Use. *Hydrocarbon Process.* **1972**, *11*, 152−156.

Table 2. Expected Uncertainties in Binary-Mixture Adsorption Measurements

system	feed gas compn (%)	total σ^a	total % σ^b	CH_4 σ^a	CH_4 % σ^b	N_2 σ^a	N_2 % σ^b	CO_2 σ^a	CO_2 % σ^b
CH_4/N_2	20/80	0.083	3.1	0.034	3.6	0.059	3.3		
	40/60	0.075	2.4	0.051	2.7	0.038	3.1		
	60/40	0.080	2.5	0.068	2.6	0.029	4.5		
	80/20	0.085	2.4	0.081	2.4	0.020	10.0		
CH_4/CO_2	20/80	0.200	3.7	0.040	17.7			0.189	3.7
	40/60	0.165	3.3	0.056	5.5			0.135	3.4
	60/40	0.159	3.5	0.078	4.1			0.098	3.7
	80/20	0.162	3.9	0.116	4.0			0.057	4.3
N_2/CO_2	20/80	0.141	2.8			0.034	39.5	0.144	2.9
	40/60	0.130	3.1			0.050	27.9	0.124	3.3
	60/40	0.124	3.5			0.059	6.6	0.100	3.8
	80/20	0.116	4.1			0.077	4.4	0.055	4.6

[a] σ is the average absolute uncertainty (mmol/g). [b] % σ is the average absolute percent uncertainty.

Table 3. Pure-Methane Adsorption on Activated Carbon at 318.2 K

run 1			run 2		
pressure (MPa)	Gibbs adsorption (mmol/g)	absolute adsorption (mmol/g)	pressure (MPa)	Gibbs adsorption (mmol/g)	absolute adsorption (mmol/g)
0.55	1.870	1.888	0.88	2.394	2.432
1.23	2.762	2.822	1.56	3.082	3.170
2.55	3.586	3.755	2.86	3.778	3.985
3.48	3.891	4.149	4.29	4.156	4.513
4.80	4.145	4.541	5.33	4.310	4.786
6.18	4.283	4.835	6.95	4.427	5.101
7.64	4.339	5.066	8.36	4.445	5.301
9.03	4.337	5.238	9.74	4.412	5.450
10.37	4.286	5.357	11.08	4.357	5.576
11.76	4.209	5.459	12.45	4.269	5.677
13.25	4.106	5.549			

Table 4. Pure-Nitrogen Adsorption on Activated Carbon at 318.2 K

run 1			run 2		
pressure (MPa)	Gibbs adsorption (mmol/g)	absolute adsorption (mmol/g)	pressure (MPa)	Gibbs adsorption (mmol/g)	absolute adsorption (mmol/g)
0.69	0.996	1.007	0.89	1.190	1.206
1.73	1.741	1.788	1.81	1.795	1.845
2.86	2.224	2.324	2.80	2.217	2.314
4.10	2.566	2.735	4.19	2.600	2.775
5.53	2.823	3.078	5.56	2.841	3.100
6.97	2.990	3.338	6.96	3.005	3.354
8.31	3.086	3.522	8.29	3.105	3.543
9.66	3.155	3.683	9.70	3.173	3.707
11.10	3.199	3.826	11.19	3.214	3.850
12.46	3.199	3.916	12.45	3.229	3.952
13.66	3.197	3.994	13.65	3.235	4.041

Gibbs adsorption. Further, the absolute adsorption of CO_2 on activated carbon is about 60% greater than that in methane and 120% greater than that in nitrogen. Also shown in the figure are the predictions of the absolute adsorption from the ZGR EOS, as is described in section 4. The selected experimental uncertainty bars are shown on the CO_2 data for illustrative purposes.

In calculating the absolute adsorption, we used a constant adsorbed-phase-density assumption. The densities employed, generated by the Ono−Kondo model,[5] are 0.354 g/cm^3, 0.701 g/cm^3, and 0.996 g/cm^3 for methane, nitrogen, and CO_2, respectively. As is shown in Table 6, the adsorbed-phase densities from the Ono−Kondo model[5] are less than the boiling-point estimates and close to the van der Waals (VDW) estimates. Also shown in Table 6 is an entry labeled "graphical estimate from the Gibbs adsorption isotherm", which is based on eq 15 and illustrated by Figure 3. As is shown in the figure for CO_2, when the absolute adsorption, $V_{ads}\rho_{ads}$, becomes constant

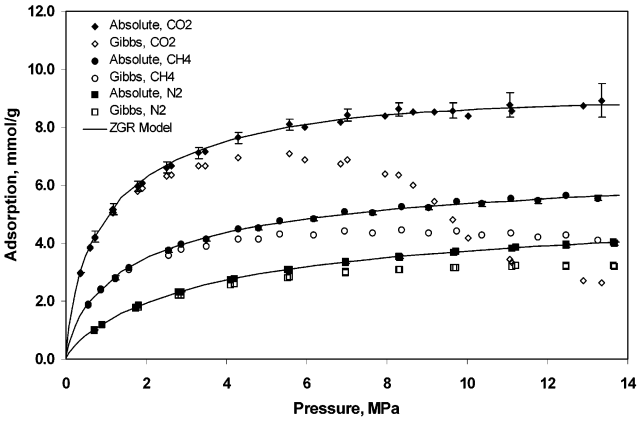

Figure 2. Pure-gas adsorption on dry activated carbon at 318.2 K.

Table 5. Pure CO_2 Adsorption on Activated Carbon at 318.2 K

run 1			run 2		
pressure (MPa)	Gibbs adsorption (mmol/g)	absolute adsorption (mmol/g)	pressure (MPa)	Gibbs adsorption (mmol/g)	absolute adsorption (mmol/g)
0.36	2.962	2.982	0.59	3.831	3.870
0.73	4.170	4.223	1.15	5.051	5.155
1.19	5.064	5.172	1.89	5.878	6.086
1.79	5.783	5.976	2.63	6.343	6.672
2.52	6.300	6.611	3.47	6.682	7.172
3.30	6.650	7.106	5.94	6.873	7.987
4.29	6.962	7.641	6.84	6.748	8.188
5.56	7.078	8.101	7.96	6.395	8.393
7.01	6.882	8.434	8.64	5.993	8.515
8.30	6.348	8.623	9.17	5.434	8.512
9.64	4.810	8.577	10.02	4.188	8.390
11.06	3.449	8.781	11.11	3.335	8.569
13.36	2.638	8.924	12.90	2.706	8.751

Table 6. Adsorbed-Phase Densities Estimated by Different Methods

method	adsorbed-phase density (g/cm^3) methane	nitrogen	CO_2
Ono−Kondo model	0.354	0.701	0.996
ZGR EOS	0.345	0.839	0.982
liquid density estimate	0.421	0.808	
solid density estimate			1.18
VDW covolume	0.374	0.725	1.03
graphical estimate from the Gibbs adsorption isotherm			1.02

at high pressures, then the Gibbs adsorption shows a linear decrease with an increasing ρ_{gas}. The extrapolation of this linear relation yields an x-axis intercept, where $\rho_{ads} = \rho_{gas}$. In this illustration, the graph indicates that $\rho_{ads} =$ 22.5 mol/L or 1.02 g/cm^3. The use of this technique requires sufficient data in the linear (high-pressure) region beyond the maximum in the Gibbs adsorption; thus, an estimate is shown in Table 6 only for carbon dioxide.

Figure 4a presents a comparison of the present data for pure CO_2 with the previous measurements of Humayun and Tomasko.[6] The measurements from their gravimetric flow apparatus are almost continuous (in frequency of acquisition), so their results appear as a continuous line in the figure. A close comparison (using a deviation plot, Figure 4b) reveals that the two data sets agree within their combined experimental uncertainties throughout most of the range of the data. This provides a very useful confirmation of both groups' experimental results. Figure 4b also illustrates that the ZGR model fits the data within their experimental uncertainties.

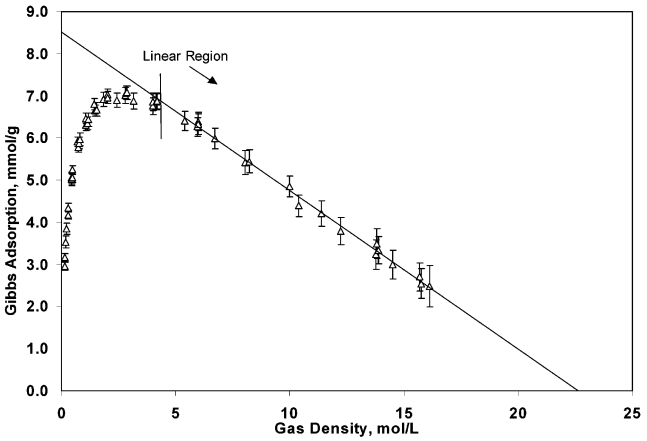

Figure 3. Graphical method for estimating the adsorbed-phase density: CO_2 adsorption on activated carbon at 318.2 K.

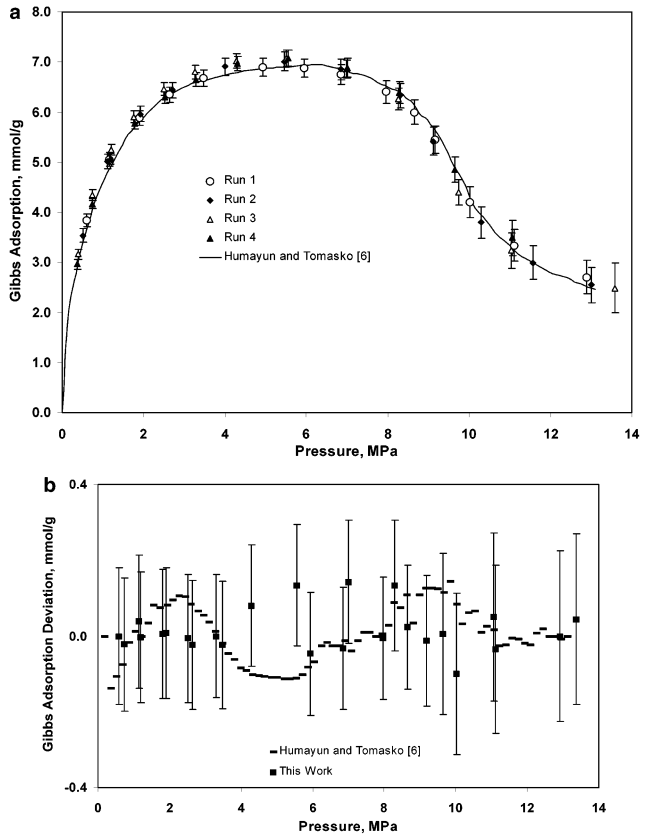

Figure 4. (a) Measurement comparison for the adsorption of pure CO_2 on dry activated carbon (b) Deviation of data from the ZGR EOS fit to the adsorption data for pure CO_2 on dry activated carbon.

3.2. Binary-Gas Adsorption. Tables 7−9 present the experimental data for CH_4/N_2, CH_4/CO_2, and N_2/CO_2 at nominal molar feed-gas compositions of 20, 40, 60, and 80% with a specific void volume ranging from 2.04 to 2.57 cm^3/g. A maximum in the Gibbs adsorption is observed for the lesser-adsorbed component at all the feed compositions, while the same phenomenon is only observed at higher feed compositions for the more highly adsorbed component. Beyond this maximum, the amount adsorbed decreases with an increasing pressure. In fact, negative values for the Gibbs adsorption of nitrogen occur at feed compositions of 40 and 20% nitrogen in the nitrogen/CO_2 system at high pressures. Physically, this means that less nitrogen is present in the adsorbed phase than would be present if the equilibrium bulk-phase gas replaced the condensed phase; this reflects the high selectivity for CO_2 over N_2 in the adsorbed phase, which leads to low nitrogen concentrations (g mol N_2/m^3) in that phase.

Table 7. Methane/Nitrogen Adsorption on Dry Activated Carbon at 318.2 K

pressure (MPa)	methane gas mole fraction	methane adsorption (mmol/g)		nitrogen adsorption (mmol/g)	
		Gibbs	absolute	Gibbs	absolute
	Methane Feed Composition, 81.7%; Specific Void Volume = 2.57 cm^3/g				
0.65	0.649	1.600	1.613	0.227	0.234
1.39	0.674	2.372	2.416	0.293	0.314
2.76	0.703	3.193	3.317	0.330	0.382
4.21	0.721	3.598	3.822	0.309	0.396
5.65	0.732	3.877	4.214	0.267	0.390
6.94	0.744	3.994	4.442	0.257	0.411
8.35	0.752	4.082	4.657	0.224	0.414
9.74	0.759	4.123	4.828	0.195	0.419
11.05	0.763	4.145	4.976	0.156	0.414
12.44	0.768	4.132	5.099	0.130	0.423
	Methane Feed Composition, 60.0%; Specific Void Volume = 2.57 cm^3/g				
0.75	0.370	1.156	1.164	0.491	0.504
1.43	0.394	1.692	1.714	0.647	0.682
2.70	0.424	2.318	2.380	0.764	0.848
4.20	0.451	2.756	2.879	0.802	0.951
5.52	0.468	3.006	3.190	0.793	1.002
6.97	0.482	3.193	3.451	0.763	1.040
8.36	0.491	3.342	3.675	0.702	1.047
9.71	0.501	3.405	3.814	0.660	1.067
11.07	0.509	3.459	3.948	0.611	1.083
12.43	0.513	3.520	4.089	0.541	1.081
	Methane Feed Composition, 40.0%; Specific Void Volume = 2.57 cm^3/g				
0.77	0.204	0.735	0.739	0.731	0.745
1.60	0.230	1.155	1.169	1.058	1.104
2.85	0.240	1.593	1.627	1.261	1.366
4.16	0.251	1.917	1.977	1.343	1.521
5.53	0.271	2.115	2.210	1.404	1.660
6.98	0.284	2.278	2.414	1.408	1.750
8.29	0.291	2.415	2.589	1.368	1.792
9.62	0.298	2.514	2.729	1.322	1.829
11.01	0.305	2.574	2.835	1.277	1.869
12.44	0.315	2.593	2.903	1.255	1.931
	Methane Feed Composition, 20.0%; Specific Void Volume = 2.57 cm^3/g				
0.76	0.094	0.326	0.328	0.915	0.929
1.50	0.100	0.520	0.525	1.348	1.389
2.77	0.106	0.754	0.766	1.754	1.856
4.16	0.112	0.942	0.965	1.987	2.169
5.55	0.119	1.075	1.112	2.116	2.386
6.95	0.128	1.158	1.211	2.200	2.560
8.36	0.131	1.248	1.317	2.213	2.669
9.70	0.137	1.292	1.379	2.231	2.777
11.07	0.143	1.317	1.424	2.232	2.870
12.44	0.147	1.348	1.473	2.210	2.940

Figures 5−10 show the absolute adsorptions of the individual components from the mixtures. For completeness, the pure-substance adsorptions are included in each figure. For each of the binary systems, the more volatile (lower critical temperature) gas is the more strongly adsorbed component only when its equilibrium gas composition is high (greater than 80% N_2 in CH_4/N_2; greater than 75% CH_4 in CH_4/CO_2; and greater than 90% N_2 in N_2/CO_2).

Dreisbach and co-workers have studied the adsorption behavior of these gases on a similar adsorbent, Norit R1 Extra activated carbon, at room temperature and pressures up to 6 MPa using a gravimetric method.[15] Their study differs in several aspects from the present work.

(15) Dreisbach, F.; Staudt, R.; Keller, J. U. High-Pressure Adsorption Data of Methane, Nitrogen, Carbon Dioxide and Their Binary and Ternary Mixtures on Activated Carbon. *Adsorption* **1999**, *5*, 215−227.

Table 8. Methane/CO_2 Adsorption on Dry Activated Carbon at 318.2 K

pressure (MPa)	methane gas mole fraction	methane adsorption (mmol/g)		CO_2 adsorption (mmol/g)	
		Gibbs	absolute	Gibbs	absolute
Methane Feed Composition, 80.0%; Specific Void Volume = 2.57 cm^3/g					
0.77	0.890	1.930	1.960	0.567	0.571
1.46	0.886	2.515	2.591	0.784	0.794
2.81	0.884	3.035	3.225	1.057	1.082
4.12	0.883	3.237	3.556	1.249	1.291
5.55	0.877	3.317	3.789	1.396	1.462
6.92	0.871	3.322	3.951	1.495	1.588
8.30	0.866	3.252	4.042	1.562	1.684
9.67	0.861	3.166	4.127	1.616	1.771
11.04	0.856	3.060	4.194	1.649	1.839
12.41	0.852	2.943	4.253	1.664	1.892
Methane Feed Composition, 60.0%; Specific Void Volume = 2.57 cm^3/g					
0.68	0.777	1.475	1.500	1.182	1.189
1.42	0.775	1.938	2.009	1.705	1.726
2.77	0.766	2.240	2.418	2.275	2.329
4.17	0.755	2.306	2.614	2.667	2.767
5.56	0.744	2.267	2.717	2.949	3.103
6.95	0.727	2.215	2.810	3.099	3.323
8.30	0.720	2.063	2.811	3.252	3.543
9.66	0.707	1.946	2.848	3.310	3.683
11.04	0.700	1.788	2.859	3.377	3.838
12.41	0.688	1.674	2.908	3.344	3.903
Methane Feed Composition, 40.1%; Specific Void Volume = 2.57 cm^3/g					
0.68	0.618	1.044	1.066	1.922	1.935
1.44	0.610	1.328	1.391	2.737	2.777
2.75	0.603	1.436	1.591	3.567	3.670
4.18	0.582	1.403	1.671	4.107	4.300
5.54	0.560	1.330	1.713	4.426	4.726
6.90	0.548	1.189	1.700	4.680	5.102
8.29	0.529	1.077	1.718	4.769	5.341
9.69	0.513	0.940	1.723	4.805	5.547
11.01	0.500	0.820	1.741	4.754	5.677
12.43	0.486	0.699	1.774	4.641	5.776
Methane Feed Composition, 20.0%; Specific Void Volume = 2.57 cm^3/g					
0.68	0.391	0.558	0.574	2.876	2.901
1.35	0.382	0.657	0.699	3.865	3.932
2.75	0.366	0.648	0.756	4.991	5.179
4.21	0.340	0.580	0.764	5.588	5.945
5.58	0.323	0.475	0.737	5.920	6.470
6.95	0.302	0.400	0.741	6.018	6.807
8.32	0.286	0.299	0.727	5.984	7.054
9.66	0.270	0.204	0.720	5.762	7.157
11.00	0.256	0.159	0.790	5.556	7.385
12.41	0.244	0.106	0.862	5.162	7.503

Table 9. Nitrogen/CO_2 Adsorption on Dry Activated Carbon at 318.2 K

pressure (MPa)	nitrogen gas mole fraction	nitrogen adsorption (mmol/g)		CO_2 adsorption (mmol/g)	
		Gibbs	absolute	Gibbs	absolute
Nitrogen Feed Composition, 80.0%; Specific Void Volume = 2.04 cm^3/g					
0.79	0.954	0.959	0.975	0.357	0.358
1.53	0.945	1.398	1.443	0.563	0.566
2.74	0.944	1.792	1.902	0.827	0.833
4.18	0.946	2.015	2.221	1.090	1.101
5.57	0.947	2.099	2.408	1.312	1.330
6.95	0.946	2.118	2.537	1.503	1.527
8.34	0.942	2.102	2.637	1.663	1.696
9.70	0.937	2.061	2.711	1.792	1.835
11.12	0.934	1.994	2.766	1.919	1.974
12.65	0.929	1.909	2.813	2.032	2.101
Nitrogen Feed Composition, 58.1%; Specific Void Volume = 2.04 cm^3/g					
0.90	0.888	0.808	0.831	0.949	0.952
1.54	0.880	1.042	1.095	1.365	1.373
2.74	0.872	1.234	1.363	1.957	1.976
4.26	0.866	1.265	1.511	2.543	2.581
5.56	0.853	1.222	1.578	2.926	2.987
6.96	0.843	1.121	1.603	3.278	3.368
8.31	0.831	1.011	1.618	3.552	3.675
9.67	0.817	0.898	1.631	3.766	3.930
11.12	0.808	0.740	1.616	3.988	4.197
12.54	0.795	0.603	1.615	4.137	4.397
Nitrogen Feed Composition, 40.0%; Specific Void Volume = 2.04 cm^3/g					
0.78	0.794	0.585	0.606	1.472	1.477
1.43	0.779	0.742	0.796	2.166	2.181
2.72	0.767	0.791	0.934	3.149	3.192
4.15	0.749	0.697	0.957	3.922	4.009
5.53	0.724	0.574	0.953	4.456	4.600
6.97	0.693	0.449	0.953	4.839	5.062
8.26	0.673	0.310	0.934	5.129	5.432
9.87	0.637	0.214	0.970	5.267	5.699
11.23	0.619	0.074	0.954	5.400	5.942
12.66	0.604	-0.080	0.937	5.521	6.187
Nitrogen Feed Composition, 20.0%; Specific Void Volume = 2.04 cm^3/g					
0.66	0.582	0.316	0.333	2.243	2.255
1.46	0.567	0.359	0.414	3.540	3.583
2.79	0.521	0.289	0.423	4.777	4.900
4.13	0.471	0.207	0.420	5.478	5.718
5.53	0.432	0.104	0.401	5.941	6.333
6.98	0.394	0.019	0.401	6.183	6.771
8.35	0.366	-0.068	0.397	6.278	7.083
9.73	0.341	-0.146	0.402	6.245	7.305
11.12	0.320	-0.232	0.405	6.122	7.475
12.52	0.299	-0.290	0.429	5.826	7.510

For the binary adsorption, they used an EOS to infer both the *bulk-phase composition* and *density* from $P-T$ measurements and system-volume calibrations, whereas we used an EOS to infer the *density* from $P-T-y$ measurements. Also, our measurements extend to much higher pressures (13.6 MPa) because at such higher pressures the adsorption data exhibit maxima for carbon dioxide and methane.[6,16−20]

4. EOS Modeling

Over the years, various researchers have applied 2-D EOS to gas adsorption. Hill[21] and de Boer[22] used the VDW EOS to correlate the pure-gas adsorptions. Hoory and Prausnitz[23] extended the 2-D VDW EOS to mixtures by introducing mixing rules. More recently, DeGance[24] used

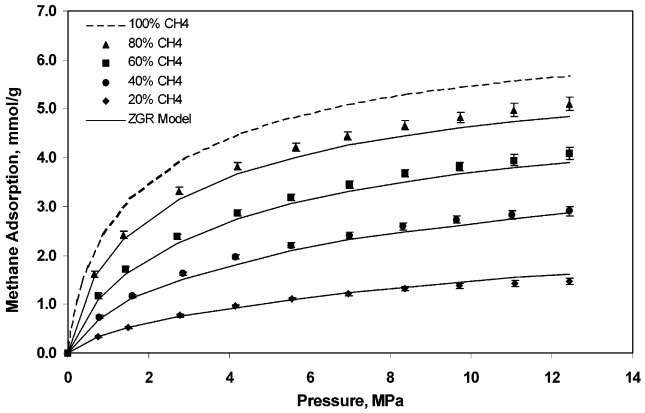

Figure 5. Absolute adsorption of methane/nitrogen on dry activated carbon at 318.2 K: methane adsorption.

(16) Benard, P.; Chahine, R. Modelling of High-Pressure Adsorption Isotherms above the Critical Temperature on Microporous Adsorbents: Application to Methane. *Langmuir* **1997**, *13*, 808−813.

(17) Chen, J. H.; Wong, D. S. H.; Tan, C. S.; Subramanian, R.; Lira, C. T.; Orth, M. Adsorption and Desorption of Carbon Dioxide onto and from Activated Carbon at High Pressures. *I&EC Research* **1997**, *36*, 2808−2815.

(18) Salem, M. M. K.; Braeuer, P.; Szombathely, M. V.; Heuchel, M.; Harting, P.; Quitzsch, K. Thermodynamics of High-Pressure Adsorption of Argon, Nitrogen, and Methane on Microporous Adsorbents *Langmuir* **1998**, *14*, 3376−3389.

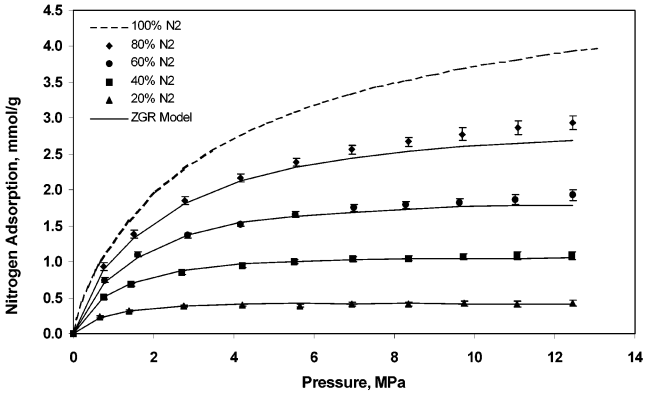

Figure 6. Absolute adsorption of methane/nitrogen on dry activated carbon at 318.2 K: nitrogen adsorption.

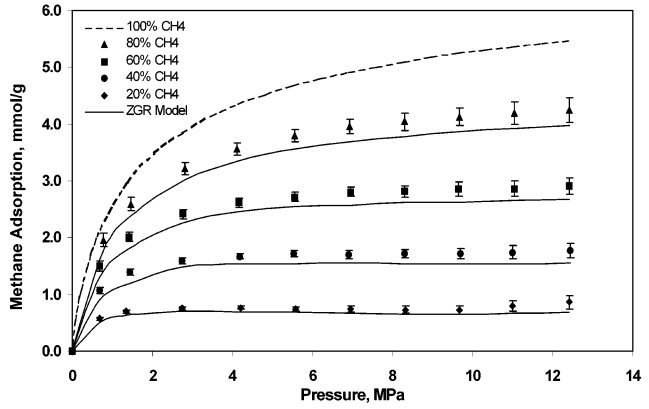

Figure 7. Absolute adsorption of methane/CO_2 on dry activated carbon at 318.2 K: methane adsorption.

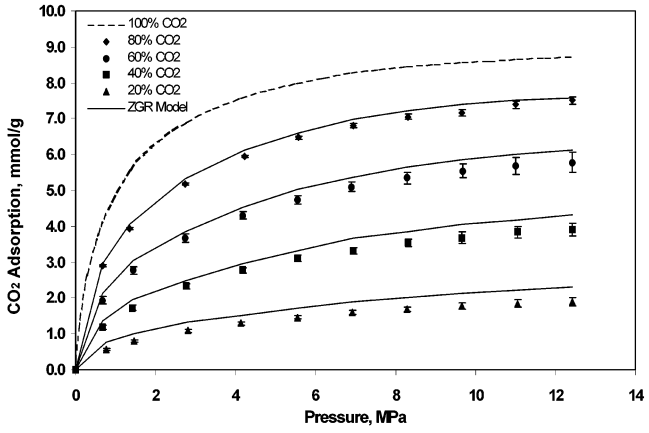

Figure 8. Absolute adsorption of methane/CO_2 on dry activated carbon at 318.2 K: CO_2 adsorption.

the 2-D virial and Eyring EOS to correlate high-pressure pure-adsorption isotherms.

In the early 1990s, we developed a generalized 2-D cubic EOS, which encompasses the 2-D analogues of all the previous cubic EOS forms.[2] The generalized 2-D EOS is analogous to the popular three-dimensional EOS used in vapor−liquid equilibrium calculations; in its generalized form

$$\left[P + \frac{a\rho^2}{1 + Ub\rho + W(b\rho)^2}\right](1 - b\rho) = \rho RT \quad (25)$$

where a and b are the traditional EOS parameters and the numerical values of U and W may be specified to give

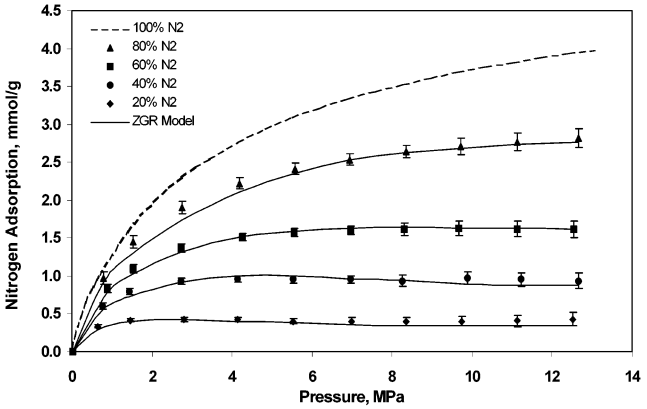

Figure 9. Absolute adsorption of nitrogen/CO_2 on dry activated carbon at 318.2 K: nitrogen adsorption.

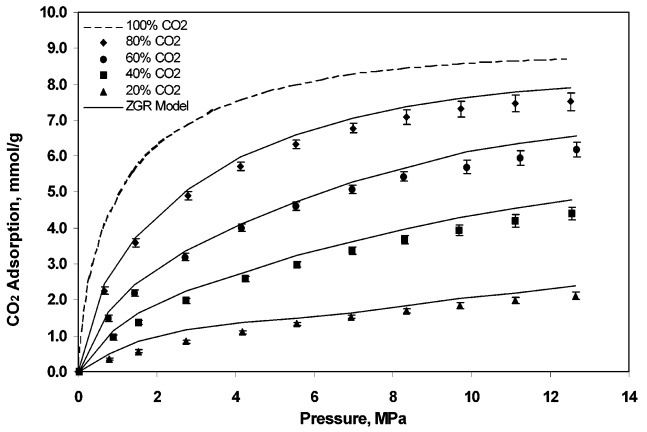

Figure 10. Absolute adsorption of nitrogen/CO_2 on dry activated carbon at 318.2 K: CO_2 adsorption.

various forms of the three-dimensional EOS. In the most general form, the 2-D analogue of the generalized cubic equation can be expressed as follows (with an additional parameter m for added model flexibility):

$$\left[A\pi + \frac{\alpha\omega^2}{1 + U\beta\omega + W(\beta\omega)^2}\right][1 - (\beta\omega)^m] = \omega RT \quad (26)$$

where A is the specific surface area, π is the spreading pressure, ω is the specific amount adsorbed (mmol/g of adsorbent), and α and β are (regressed) model parameters. The model coefficients U, W, and m must be specified to obtain a specific form of the 2-D EOS for application. For example, an analogue of the VDW EOS is obtained by setting $m = 1$ and $U = W = 0$ and is similarly obtained for the Soave−Redlich−Kwong ($m = U = 1$ and $W = 0$),

(19) Katsuyuki, K.; Mustapha, E.-M.; Katsumi, K. A New Determination Method of Absolute Adsorption Isotherm of Supercritical Gases Under High Pressure with a Special Relevance to Density-Functional Theory Study. *J. Chem. Phys.* **2001**, *114*, 4196−4205.

(20) Malbrunot, P.; Vidal, D.; Vermesse, J.; Chahine, R.; Bose, T. K. Adsorption Measurements of Argon, Neon, Krypton, Nitrogen, and Methane on Activated Carbon up to 650 MPa. *Langmuir* **1992**, *8*, 577−580.

(21) Hill, T. L. Theory of Multimolecular Adsorption From a Mixture of Gases. *J. Chem. Phys.* **1946**, *14*, 268.

(22) de Boer, J. H. *The Dynamical Character of Adsorption*; Oxford University Press: London, 1953.

(23) Hoory, S. E.; Prausnitz, J. M. Monolayer Adsorption of Gas Mixtures on Homogeneous and Heterogeneous Solids. *Chem. Eng. Sci.* **1967**, *22*, 1025.

(24) DeGance, A. E. Multicomponent High-Pressure Adsorption Equilibria on Carbon Substrates: Theory and Data. *Fluid Phase Equilib.* **1992**, *78*, 99.

Peng−Robinson ($m = 1$, $U = 2$, and $W = -1$), and Eyring ($m = {}^1/_2$ and $U = W = 0$) EOS.

This general 2-D EOS can be used to investigate EOS behaviors by specifying various combinations of model coefficients. The model coefficient m has been found to be the most important among the EOS model coefficients because it has a significant effect on the shape of the pure-adsorption isotherm. If U and W are equal to 0, then by setting m to values of 1 and ${}^1/_2$, we obtain the 2-D VDW EOS and the Eyring EOS, respectively.

Actually, the pure-gas isotherms vary considerably in shape and Zhou et al.[2] found that it is sometimes desirable to select an m value even smaller than ${}^1/_2$ to describe pure isotherms. They determined that an equation with $m = {}^1/_3$ and $U = W = 0$ (the ZGR EOS) showed considerable promise and the 2-D EOS could be applied to the adsorbed phases containing mixtures by utilizing the traditional mixing rules (where x is the mole fraction in the adsorbed phase)

$$\alpha = \sum_i \sum_j x_i x_j \alpha_{ij} \tag{27}$$

$$\beta = \sum_i \sum_j x_i x_j \beta_{ij} \tag{28}$$

along with the nontraditional combination rules

$$\alpha_{ij} = (1 - C_{ij})(\alpha_i + \alpha_j)/2$$
$$\beta_{ij} = \sqrt{\beta_i \beta_j}(1 + D_{ij}) \tag{29}$$

where C_{ij} and D_{ij} are the empirical binary-interaction parameters.

The absolute adsorption of the pure- and binary-gas systems was correlated with the 2-D ZGR EOS, which is described in detail elsewhere.[2] The equilibrium between the adsorbed phase and gas phase will lead to the following relation:[2]

$$A x_i \pi \hat{\phi}_i^{\mathrm{a}} = k_i R T \hat{f}_i^{\mathrm{g}} \tag{30}$$

where $\hat{\phi}_i^{\mathrm{a}}$ is the fugacity coefficient in the adsorbed phase obtained from the 2D EOS model, $\hat{f}_i^{\mathrm{g}}$ is fugacity in the gas phase obtained from the 3D EOS, and k_i represents the slope of the pure-component (ω versus P) isotherm at the origin. For the ZGR EOS, the fugacity expression is

$$\ln \hat{\phi}_i^{\mathrm{a}} = \frac{2\sum_j \beta_{ij}\omega_j - \beta\omega}{(\beta\omega)^{1-m} - \beta\omega} - \frac{1}{m}\ln[1 - (\beta\omega)^m] - \ln Z_{\mathrm{a}} - \frac{2}{RT}\sum_j \alpha_{ij}\omega_j \tag{31}$$

where $Z_{\mathrm{a}} = \pi A/\omega RT$. In the present work, the gas-phase fugacities were calculated using a modified Redlich−Kwong EOS.[2]

Table 10. ZGR EOS Representation of Pure-Gas Adsorption on Dry Activated Carbon at 318.2 K

	regressed parameters				
component	α	β	ln k	NPTS[a]	% AAD[b]
methane	8.1826×10^3	0.081 454	1.222 64	21	0.5
nitrogen	1.2231×10^4	0.106 498	-0.002 72	22	0.4
CO_2	4.7611×10^3	0.049 399	2.155 19	22	1.4

[a] NPTS = number of data points evaluated. [b] % AAD = average absolute percent deviation.

Table 11. ZGR EOS Representation of Binary Mixed Gas Adsorption on Dry Activated Carbon at 318.2 K

		% AAD[a]			regressed parameters	
system	NPTS	comp. 1	comp. 2	total	C_{ij}	D_{ij}
CH_4/N_2	40	4.6	3.1	3.6	-0.0247	0.0209
CH_4/CO_2	40	8.6	9.5	1.2	0.1061	-0.0097
N_2/CO_2	40	5.4	10.8	4.6	0.2495	-0.1657

[a] % AAD = average absolute percent deviation.

The regressions used to determine the model coefficients minimized the sum of the squares of the relative errors in the predicted amounts adsorbed. The optimized parameters included α and β for each pure component, as well as k (in eq 30) for each pure system and the interaction parameters C_{ij} and D_{ij} for each binary system.

Figure 2 shows the 2-D ZGR-EOS representations of the pure-component adsorptions. The model shows an excellent fit, within the experimental uncertainties. Table 10 presents the parameters used to fit the pure-adsorption data.

The parameters obtained from the pure adsorption, plus the two optimized binary-interaction parameters, were used to represent the binary-adsorption data. Table 11 contains the binary-interaction parameters used for these mixtures. Figures 5−10 show the model representations for the component adsorptions of the binary systems studied. The figures show that the model represents the mixture data within 1−2 times the experiment uncertainties. We anticipate that the representation of the data can be improved, however, by the use of improved mixing rules in the ZGR EOS modeling and inclusion of nonideal mixing rules for the adsorbed phase density in the data reduction (in place of eq 21).

5. Conclusion

The adsorption of methane, nitrogen, CO_2, and their binary mixtures was measured on dry activated carbon at 318.2 K and pressures up to 13.6 MPa using a volumetric/gas chromatographic method. Both the Gibbs and the absolute-adsorption results are presented. The ZGR EOS is shown to be capable of describing the pure-component data within their experimental uncertainties and the mixture data within 1−2 times the expected uncertainties. Finally, the data for CO_2 are recommended as a reference data set for the evaluation of experimental apparatus/techniques for measuring high-pressure adsorption from supercritical gases.

LA020976K